Detection of *BRAF* V600E Mutations With Next-Generation Sequencing in Infarcted Thyroid Carcinomas After Fine-Needle Aspiration

Erik Kouba, MD,[1] *Andrew Ford, MS,*[2] *Charmaine G. Brown,*[2] *Chen Yeh, PhD,*[2] *Gene P. Siegal, MD, PhD,*[1] *Upender Manne, PhD,*[1] *and Isam-Eldin Eltoum, MD, MBA*[1]

From the [1]Department of Pathology, University of Alabama–Birmingham; and [2]Circulogene, Birmingham, AL.

Key Words: *BRAF* V600E; Thyroid carcinoma; Next-generation sequencing; Fine-needle aspiration; Fine-needle aspiration infarction

Am J Clin Pathol August 2018;150:177-185

DOI: 10.1093/AJCP/AQY045

ABSTRACT

Objectives: *Fine-needle aspiration (FNA) of thyroid lesions may result in infarction and diagnostic difficulties on subsequent thyroidectomy specimens. Next-generation sequencing (NGS) methods for detection of hallmark driver* BRAF *V600E mutations may help characterize such tumors in which histologic alterations preclude definitive tissue diagnosis.*

Methods: *Thyroidectomy specimens with both malignant FNA diagnoses and resultant infarction were identified from our institutional database. NGS methods were used to detect* BRAF *V600E mutations in the infarcted thyroid carcinomas.*

Results: *Nine thyroid carcinomas with infarction were characterized as* BRAF*-like papillary thyroid carcinoma based on molecular driver categorization and histologic diagnosis.* BRAF *V600E mutations were detected in the infarcted tissue in four (67%) of six lesions.*

Conclusions: *We demonstrate detection of hallmark* BRAF *V600E mutations by NGS within infarcted tissue of thyroid carcinomas after FNA. This suggests a potential ancillary method of characterizing infarcted thyroid carcinomas whose altered histology may be nondiagnostic.*

Thyroid cancer is the most common malignancy of endocrine organs, with an estimated 56,870 new cases and 2,010 deaths in the United States in 2017.[1,2] Most tumors arise from follicular cells, and appropriate treatments allow a 5-year overall survival of 97.7%. The classical genetic alterations in these carcinomas includes four genes involved in the mitogen-activated protein kinase pathway, including *BRAF* and *RAS* (point mutations) and *RET*/*PTC* and *PAX8*/*PPARγ* (gene rearrangements). Most recently, genomic studies have classified differentiated thyroid carcinomas based on oncogenic driver subtypes: *BRAF*-like, *RAS*-like, and non-*BRAF*-like non-*RAS*-like.[3-5] For *BRAF*-like carcinomas, the most prevalent somatic *BRAF* mutation involves substitution of glutamic acid for valine at position 600 in the *BRAF* gene (*BRAF* V600E) with prevalence in up to 90% of conventional papillary thyroid carcinomas (PTCs), 85% of PTC tall cell (TC-PTC) variants, and 20% of PTC follicular (FV-PTC) variants.[2] As such, detection of *BRAF* V600E mutations may provide diagnostic utility in clinical management of thyroid carcinomas.[6-10] The method for detection of genetic mutations has evolved from conventional polymerase chain reaction (PCR) and Sanger sequencing requiring fresh-frozen tissue toward next-generation sequencing (NGS) methods using either preserved aspirates or formalin-fixed specimens.[11-13]

Clinical evaluation of palpable thyroid nodules follows the 2015 guidelines of the American Thyroid Association (ATA) and incorporates both ultrasound features and fine-needle aspiration and cytology (FNAC).[2,14] Cytologic diagnosis uses standardized diagnostic criteria

based on the Bethesda System for Reporting Thyroid Cytopathology (2006).[15] For the six diagnostic categories, each is associated with a risk of malignancy that guides subsequent clinical management.[16,17] Based on the aforementioned, clinical management of thyroid nodules may entail observation, repeat aspiration (with genetic testing), or thyroidectomy.[18]

Although fine-needle aspiration (FNA) remains the diagnostic procedure of choice, the phenomenon of post-biopsy infarction and necrosis of the thyroid nodule has been described by others in a few small case series and case reports.[19-22] FNA trauma can disrupt the rich microvasculature network of the benign parenchyma and neovascularized tumor. Such trauma can lead to altered tissue architecture, cystic degeneration, capsule disruption, and papillary endothelial hyperplasia. Difficulties in diagnosis may subsequently occur in relation to such histologic alterations, in addition to capsular pseudoinvasion, reactive nuclear atypia, and spindle cell proliferations.[20,23-25] Moreover, the degree of tissue infarction varies and oftentimes only spares a minute rim of epithelial tissue at the periphery. In cases with complete obliteration, the absence of epithelial elements can render a pathologic diagnosis impossible, in turn, thwarting subsequent clinical management.[20-22,24,26]

In view of such potential diagnostic dilemmas, this single-institution study examined the histologic alterations in nine cases of thyroid carcinoma with post-FNA infarction. Moreover, we used NGS for detection of *BRAF* V600E mutations in the infarcted regions to examine the potential of molecular tumor characterization when absent histologic features preclude diagnosis. This study comprises a single institutional series characterizing malignant post-FNA lesions and demonstrates the potential utility of detection of *BRAF* V600E gene mutations in infarcted tissue.

Materials and Methods

Study Specimens

With approval by our institutional review board, we retrospectively reviewed our surgical files between 2010 and 2015 and identified nine patients who underwent thyroidectomy with a subsequent diagnosis of thyroid carcinoma with infarct. All patients had prior evaluation of thyroid nodules in accordance with the ATA guidelines for management of thyroid lesions at our institution.[14] Staff radiologists performed Doppler ultrasound-guided FNA using a standard method of five to six passes using a 22- or 25-gauge needle without vacuum syringe suction. Cytologic evaluation and diagnosis was based on criteria set forth by the 2006 Bethesda System for Reporting Thyroid Cytopathology by a board-certified cytopathologist.[15] After surgical extirpation of the thyroid gland, prognostic pathologic findings were identified using criteria of the 2017 American Joint Committee on Cancer (eighth edition).[27]

Histopathologic Characterization

The available H&E-stained slides for each of the nine cases were re-reviewed in a blinded fashion to determine the extent of tumor infarction. In addition, the tumor was characterized based on histologic criteria for reactive and reparative changes found in acute (<3 weeks) and chronic (>3 weeks) periods.[19,20,28] The extent of infarction of lesions was determined and categorized as complete (>99%), near total (90%-99%), or extensive (60% to <90%).[23] Clinical variables included age and sex, cytologic diagnosis, and time interval from FNA to surgery. Pathologic variables included surgical procedure, tumor type, size, tumor laterality, extrathyroidal extension into soft tissue, presence or absence of vascular invasion, and presence or absence of nodal metastases.

DNA Extraction

From the H&E-stained slides, regions from the infarcted regions, corresponding tumor, and peritumoral tissue were selected for molecular characterization. This region of interest was transferred to corresponding formalin-fixed, paraffin-embedded (FFPE) blocks using corresponding tissue slides and stereotactic landmarks. A complete core of infarcted tumor was obtained using a full-thickness 1-mm punch biopsy of the block. In each case, the core location was confirmed using a postsampling H&E slide **Image 1**. Genomic DNA was extracted from the FFPE tissue punch using the commercially available AllPrep DNA/RNA FFPE Kit (Qiagen, Venlo, The Netherlands). Briefly, tissue cores were subjected to xylene treatment for paraffin extraction from the tissue and then rehydrated using a 100% ethanol wash. After the centrifugation, the pellet was resuspended in proteinase K buffer (>600 mAU/mL solution). Protein and enzymes such as nucleases were subsequently digested by proteinase K. The entire sample was transferred to a QIAamp MinElute spin column (Qiagen). The specimen was centrifuged for 15 seconds at 8,000*g* (≥10,000 rpm) to wash the spin column membrane. Afterward, it was transferred to the QIAamp MinElute spin column in a new 1.5-mL collection tube. A 30- to 100-µL volume of elution buffer was added directly to the spin column membrane and incubated for 1 minute at room

DOI: 10.1093/ajcp/aqy045

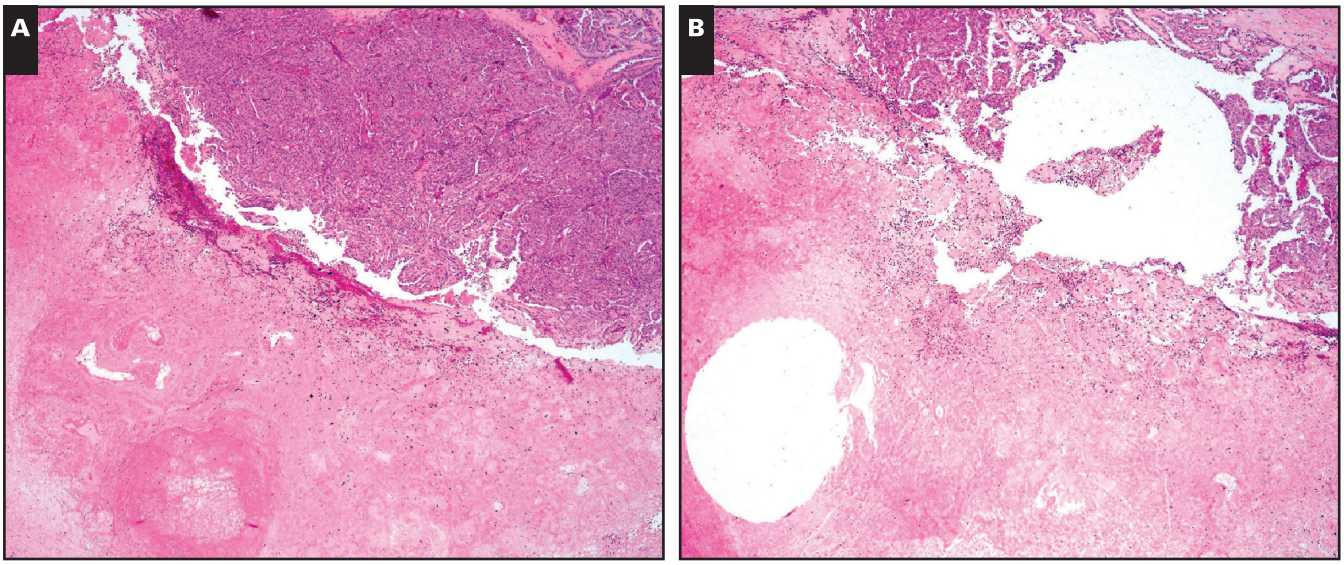

Image 1 Representative postcore 1-mm punch sites. **A**, Case 2, prepunch sites, infarct lower left corner, rim of papillary thyroid carcinoma (PTC) upper right corner. **B**, Case 2, core postpunch sites, infarct lower left corner, rim of PTC upper right corner. (H&E, ×100)

temperature. Last, the specimen was centrifuged at full speed for 1 minute to elute the DNA.

Detection and Classification of Genetic Mutations

Quantification of complementary DNA (cDNA) was performed using the Qubit 2.0 fluorometer together with double-stranded DNA broad range and high sensitivity assay kits (Life Technologies, Carlsbad, CA). Deep targeted sequencing and data analysis were next carried out using Ion Torrent NGS (Thermo Fisher Scientific, Waltham, MA). Briefly, the targeted sequencing libraries were generated using the Ion AmpliSeq Library Kit 2.0 and Cancer Hotspot Panel v2 according to the manufacturer's instructions (Life Technologies). The starting material consisted of 1 to 20 ng cDNA. Each sample was analyzed for the entire 50-gene panel interrogating a total of approximately 3,000 mutations. The primers used for library amplification were then partially digested by Pfu enzyme followed by ligation with corresponding molecular barcoded adapters and subsequently purified using Ampure beads (Beckman Coulter, Beverly, MA). The quality of the libraries was assessed using quantitative real-time PCR. Then, 70 to 100 picomolar of each library was loaded onto the Ion Chef system (Thermo Fisher Scientific) for emulsion PCR to clonally amplify sequencing templates. Ultra-deep sequencing was performed on the Ion Torrent Proton Instrument with an average coverage of greater than ×5,000. Sequencing data were analyzed by the Variant Caller 4.2 software (Ion Torrent, Thermo Fisher Scientific) using somatic high-stringency parameters and the targeted and hotspot pipelines. All the variants identified were further confirmed by analyzing the data through GenePool (Station X, San Francisco, CA). Thyroid carcinomas were classified based on the following oncogenic drivers: *BRAF*-like, *RAS*-like, and non-*BRAF*-like non-*RAS*-like. *BRAF*-like carcinomas were defined by detection of the *BRAF* V600E gene mutation in the tumor or peritumoral tissue. Similarly, *RAS*-like carcinomas were defined by detection of known *RAS* gene mutations. In addition, the most common genetic mutations related to de-differentiation were noted within each category of oncogenic driver-type carcinoma.[3,4,13,29]

Results

FNAC

The cohort consisted of two men and seven women with a mean (median) age of 53 (55) years. The mean (median) ultrasound measurements of the tumors were 28 (21) mm; two cases were less than 1 cm. Seven of nine were solid while two contained a cystic component. Five tumors were in the left lobe, three were located in the right lobe, and one was located midline. FNA was performed once in eight patients, and repeat biopsy was carried out in one patient (initial FNA performed 200 days prior at an outside institution). The cytology findings according to the Bethesda classification were as follows: malignancy-PTC (six cases), suspicious for PTC (one case), atypia

DOI: 10.1093/ajcp/aqy045

of undetermined significance (one case), and necrosis (one case; the patient had a prior partial thyroidectomy for a pathologically diagnosed PTC) **Table 1**.

Surgical Pathology: Characteristics and Diagnoses

All patients underwent surgical extirpation by either a total thyroidectomy in seven (78%) patients, right hemi-thyroidectomy in one (11%) patient, and midline mass excision in one (11%) patient. The mean (median, range) interval from last FNA to surgery was 35 (38, 2-69 days, respectively). The mean (median) pathologic size of lesions was 28 (25) mm. Despite the extent of infarction, there was adequate viable tissue whose morphologic features allowed pathologic diagnosis to be rendered. The final pathologic diagnoses were conventional PTC (PTC) in five lesions, TC-PTC in two lesions, FV-PTC in one lesion, and poorly differentiated thyroid carcinoma (PD), including insular, in the final lesion **Table 2**.

Most tumors contained high-risk pathologic features: six of nine cases demonstrated extra-thyroidal extension (pT3); case 5 had extension into the tracheal cartilage (pT4). In addition, vascular invasion was identified in one of nine cases. Lymph node metastases were identified in four of nine cases, with three cases having regional nodal metastasis (pN1b) and one case (case 8) demonstrating central compartment nodal metastases (pN1a). Case 1 (FV-PTC) contained no high-risk features (Table 2).

Degree of Lesion Infarction and Histologic Alterations

The five lesions with extensive infarction (60% to <90% of lesion) comprised the largest tumor cohort within the series (25-65 mm; mean, 46 mm). The time from FNA to surgery for these five patients showed a wide range (14-53 days; mean, 34 days). These five lesions comprised all PTC subtypes. For the two lesions with near-total infarction (90%-99%), size tended to be smaller (4 and 10 mm). The time interval from FNA to surgery was similar to the other cases; the 2-day interval in case 5 represented urgent surgical intervention. The two cases with complete infarction (cases 1 and 7) were the smallest lesions (1 and 6 mm), with the longest interval from FNA to surgery (69 days) (Table 1, Table 2, and **Table 3**).

The tissue alterations within the infarcted zones showed the temporal features of thyroid tissue injury patterns reported by others.[23-25] Most cases showed evidence of recent and old hemorrhage and early granulation tissue repair expected in the acute period postinfarct (<3 weeks). Fibrosis and hemosiderin would be expected in older infarcted lesion as reported in the literature (>3 weeks).[19-21,28,30] All cases with dystrophic calcification had post-FNA intervals reflecting tissue alterations of the chronic postinfarct period (>3 weeks). Furthermore, two cases showed osseous metaplasia, another feature of chronic change. Case 7 showed additional features associated with late tissue alterations and corresponded to the longest interval from surgery (69 days). Case 4 also showed these features, but the osseous formation was thought to be related to the presence of poorly differentiated thyroid carcinoma rather than being solely based on postinfarct alterations (Table 3 and **Image 2**).

Genetic Mutations

NGS identified *BRAF*-like carcinomas in six of nine cases. For these tumors, *BRAF* V600E mutations were also found in the infarcted tissue in four (67%) of six cases. Case 4 was classified as *RAS*-like with detection of mutation *HRAS* Q61R. Two cases (cases 7 and 9) were classified as non-*BRAF*-like non-*RAS*-like. The *BRAF* V600E mutation was identified in three (60%) of five cases of PTC, two (100%) of two cases of TC-PTC, and in the one case of FV-PTC. Cases with detectable *BRAF* V600E mutations showed no apparent relation to the degree of infarction. Regarding high-risk pathologic characteristics, most *BRAF*-like carcinomas had

Table 1
Clinicopathologic Variables

Case No.	Sex/Age, y	Size, mm	Location	Cytologic Diagnosis	No. of FNA Procedures	FNA to Surgery, d
1	M/37	6	R	PTC	1	27
2	F/55	10	L	PTC	1	38
3	F/21	25	L	SUSP-PTC	1	53
4	F/59	55	R	AUS	1	41
5	F/74	4	M	Necrosis	1	2
6	F/88	65	L	PTC	1	37
7	F/43	1	L	PTC	1	69
8	F/57	25	R	PTC	2	26
9	M/46	60	L	PTC	1	14

AUS, atypia of undetermined significance; FNA, fine-needle aspiration; L, left; M, midline; PTC, papillary thyroid carcinoma; R, right; SUSP PTC, suspicious for papillary thyroid carcinoma.

DOI: 10.1093/ajcp/aqy045

Table 2
Pathologic Variables and *BRAF* V600E Mutation Detection

Case	Pathologic Diagnosis	ETE	Vascular Invasion	Nodal Metastasis	*BRAF*-Like Tumor	*BRAF* V600E Mutation in Infarct
1	FV-PTC	N	N	N	Y	Y
2	PTC	Y	N	N	Y	N
3	TC-PTC	Y	N	Y	Y	Y
4	PD	Y	Y	N	N	NA
5	PTC	Y	N	N	Y	Y
6	TC-PTC	Y	N	Y	Y	N
7	PTC	N	N	N	N	NA
8	PTC	N	N	Y	Y	Y
9	PTC	Y	N	Y	N	NA

ETE, extrathyroidal extension; FV-PTC, follicular variant of papillary thyroid carcinoma; N, no; NA, not applicable; PD, poorly differentiated thyroid carcinoma, including insular; PTC, papillary thyroid carcinoma; TC-PTC, tall cell variant of papillary thyroid carcinoma; Y, yes.

one or more findings except for the FV-PTC. However, compared with the non *BRAF*-like tumors, there were no apparent differences. Unfortunately, the limited number of specimens precludes true statistical comparison and definitive conclusions (Table 2).

Additional genetic mutations associated with de-differentiation were identified in two cases. Case 5 contained both *BRAF* V600E mutations and the mutated oncogene *PIK3CA* I391M. These two mutational combinations comprise phenotypes associated with rapidly lethal anaplastic thyroid carcinoma in murine models.[31] Moreover, the distinct genetic combination has been identified in genomic sequencing of anaplastic thyroid carcinoma in humans.[32] Although the patient had a small focus of PTC identified in the resection specimen (in a background of infarcted, necrotic tissue), the aggressive clinical behavior (tracheal invasion) supports the possibility of anaplastic carcinoma and is in favor with the genotyping.[31-35] Similarly, case 4 showed the detection of the combination of driver mutation *HRAS* Q61R and the mutated oncogene *PIK3CA* I391M, which has also been characterized in other series as an aggressive phenotype with potentially fatal outcomes. This genotype is in keeping with the poorly differentiated histologic features and high-risk pathologic characteristics.[32,35-37]

Discussion

Infarction of papillary thyroid lesions after FNA is a rare but recognized occurrence, with approximately 24 cases reported as of 2014.[20,24] These published cases are well summarized by Kholová[22] and Liu et al.[20] Mechanisms related to procedural methods may contribute to increased tissue damage, including needle size, vacuum aspiration, FNA without radiologic guidance, and multiple passes, among others.[20,22,24] Other potential variables include features inherent to the lesion, including Hürthle cell changes, cystic regions, and Hashimoto thyroiditis.[23,26,38] Regardless of the mechanism, post-FNA infarction can obscure tumor cells, making accurate pathologic diagnosis difficult. Although FNA may yield an accurate cytologic diagnosis, the conundrum of a vanished tumor after surgery can be profound.[38] Methods to salvage a diagnosis of an infarcted tumor with a high

Table 3
Histologic Tissue Alterations in Infarcted Thyroid Nodules[a]

		Tissue Changes					
Case No.	Infarct Extent	Recent Hemorrhage	Hemosiderin	Granulation Tissue	Fibrosis	Dystrophic Calcification	Osseous Metaplasia
1	Complete	+	+	+	+	–	–
2	Near total	+	+	+	+	+	–
3	Extensive	+	+	+	+	+	–
4	Extensive	+	–	+	+	+	+
5	Near total	+	+	+	+	–	–
6	Extensive	+	–	–	+	+	–
7	Complete	–	–	–	+	+	+
8	Extensive	+	+	+	+	+	–
9	Extensive	+	+	+	+	–	–

+, present; –, absent.
[a]The extent of lesion infarction categorized as complete (>99%), near total (90%-99%), or extensive (60% to <90%).

DOI: 10.1093/ajcp/aqy045

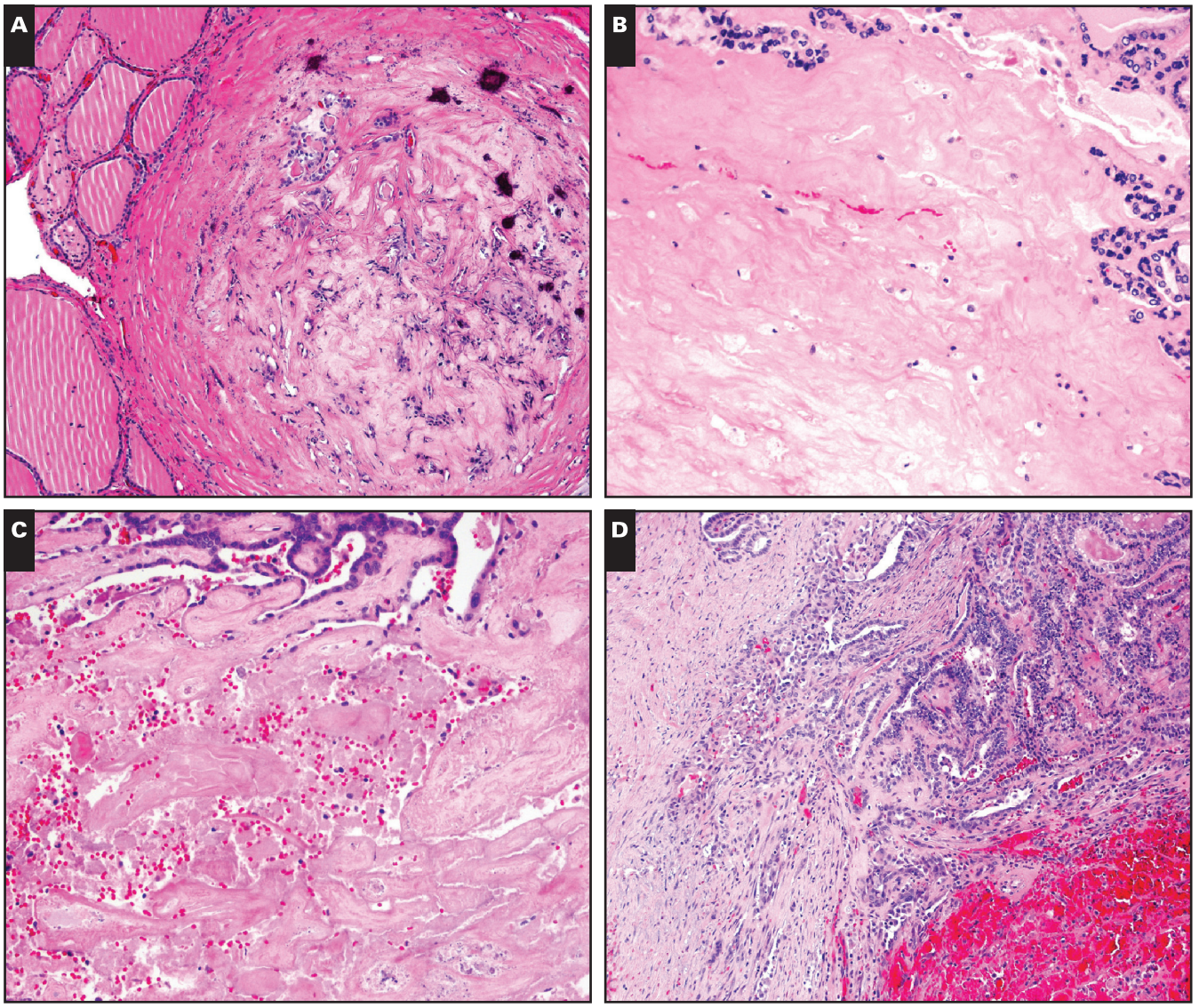

Image 2 Representative regions of infarction. **A**, Case 7, fibrosis, hemosiderin, dystrophic calcifications. **B**, Case 5, dense fibrosis residual tumor left upper corner. **C**, Case 3, fresh hemorrhage, fibrosis. **D**, Case 8, fresh hemorrhage, granulation tissue, faint hemosiderin. (H&E, ×100)

preresection probability of carcinoma have included immunohistochemical stains, interpretation of "ghost" cells, and identification of subtle clues such as psammomatous calcifications; however, interpretation may still be limited by the altered tissue architecture, cystic degeneration, capsule disruption, papillary endothelial hyperplasia, and questionable staining patterns. Several cases have reported that such diagnostic dilemmas have been remedied by the identification of metastatic PTC.[21-23,26,39]

To our knowledge, molecular analysis of the infarcted tissue has not been used in such circumstances. Eze et al[21] reported the presence of *BRAF* V600E mutations from an FNA procedure, but no attempts at characterization of the infarcted material were attempted. Similarly, Bhatia et al[28] reported FNA genetic expressions from Afirma testing (Veracyte, South San Francisco, CA), but such a method is inadequate for postresection tissue characterization. Therefore, this study attempted to identify thyroid carcinoma by detection of the oncogenic driver *BRAF* V600E mutation using NGS methods that have been recently implemented in thyroid oncology with the capability to detect not only single characteristic genetic alterations such as *BRAF* V600E but also hundreds of additional genes of interest.[12,40] With this technology, detection of *BRAF* V600E mutations has already been integrated into the algorithmic diagnosis of PTC in thyroid nodules with either indeterminate cytologic diagnoses or in nodules with worrisome ultrasound features.[9,41-44]

DOI: 10.1093/ajcp/aqy045

In this series, six of nine tumors were classified as *BRAF*-like thyroid carcinoma based on detection of *BRAF* V600E mutations.[32] In these tumors, the *BRAF* V600E mutation was detected in the infarcted region in four (67%) of six cases. As such, detection of *BRAF* V600E mutations by NGS may provide a means for identifying potential genetic fingerprints of residual DNA in such vanished tumors. As aforementioned, *BRAF* V600E mutations are highly prevalent in PTC and many subtypes, with variation among populations (40%-90%).[45,46] The limits of detection for NGS methods allow characterization of DNA using small quantities of tissue from FFPE specimens.[12] The *BRAF* V600E mutation demonstrates minimal tumoral heterogeneity and has also been identified in the peritumoral tissue. Moreover, the somatic mutation is mutually exclusive for other neoplasms of the head and neck (excluding skin) and is absent in normal thyroid glands.[3,13,29,47,48] In other words, *BRAF* V600E mutation is highly specific for the diagnosis of thyroid carcinoma. This study extends the capability of NGS in the detection of *BRAF* V600E mutations in tissue with histologic alterations after FNA-related infarction.

Like other series, our study comprises a wide range of nodule sizes (1-65 mm), wide range of intervals of FNA to surgery (2-69 days), and varied degrees of infarction (complete to extensive). The age range and sex of patients also reflect the demographics of previously reported series. However, our cohort is unique in that all patients underwent a preoperative FNA procedure and cytologic diagnosis at our institution by a standardized method. Other series have included specimens obtained using unknown FNA methods at outside institutions with oftentimes questionable cytology. Furthermore, other series have included infarctions occurring in mimickers of PTC, including Hürthle cell neoplasms, chronic lymphocytic thyroiditis, and nodular hyperplasia.[20,22,24-26,28]

The postinfarct histology of the cases demonstrates tissue alterations consisting of a temporal tissue injury pattern (ie, both acute and chronic) as reported by others (Image 2). Most cases showed evidence of recent and old hemorrhage and early granulation tissue repair expected in the acute period postinfarct (<3 weeks) (Table 3). The study cohort also included a wide degree of infarction, including complete, near complete, and extensive. Identification of the tumor was often found along the rim of the infarct after meticulous examination of deep levels, a finding also published by others. In this study, a tissue diagnosis was made in all cases.[22,24]

Most of the cases in the present study showed aggressive pathologic features, including extrathyroidal extension (six of nine cases), vascular invasion (one of nine cases), and nodal metastasis (four of nine cases). Unfortunately, previous studies have not reported such pathologic details of resected lesions, making comparison difficult. Moreover, it remains uncertain whether the underlying biology of the tumor may also contribute to infarction and degree of subsequent fibrosis. The plausibility of such influences in *BRAF* V600E carcinoma is supported by studies that highlight the complex functional links related to angiogenesis and stromal fibrosis. For example, *BRAF* V600E thyroid carcinomas show increased microvascular density, increased vascular endothelial growth factor, and increased hypoxia-inducible factor-α compared to *BRAF* wild-type carcinomas. In addition, the stromal elements show upregulated activity of cancer-associated fibroblasts, especially in tumors with *BRAF* V600E mutations. The upregulated stromal activity is also highlighted by additional upregulation of genes associated with stromal collagen deposition and extracellular matrix.[49-51]

The use of NGS in the current study identified two infarcted thyroid carcinomas (both *BRAF*-like and *RAS*-like) with known de-differentiation genetic mutations associated with poorly differentiated and anaplastic thyroid carcinoma. Interestingly, for the de-differentiated *BRAF*-like tumor, the pathologic diagnosis did not correlate with the aggressive biological behavior as predicted by the phenotype. Conversely, the PD thyroid carcinoma (case 5) had a de-differentiated *RAS*-like genetic profile consistent with PD carcinoma with concordant morphologic features and subsequent pathologic diagnosis. Like differentiated thyroid carcinoma, it is unknown as to whether tumor biology may contribute to post-FNA infarction. Studies suggest similar alterations in the stromal microenvironment with increased cancer-associated fibroblast-mediated collagen remodeling and extracellular cellular matrix modifications with potential rapid progression of tumorigenesis.[31,32,49,50,52,53] It also is tempting to speculate that other subtypes may also possess de-differentiating genetic mutations with a resultant phenotype prone to infarction. Future studies are needed to characterize thyroid carcinomas for such genomic and transcriptional hallmarks in infarcted tumors.

The major limitations of this study include the small sample size (inherent in studies of uncommon entities) and the retrospective design, including the known potential for selection bias, recall bias, and potential impact of unknown confounding variables. In this study, the effects of selection bias and analytical bias were minimized by blinded methods of tissue selection and blinded NGS analysis using commercial kits with sequential batch analyses. The effects of recall bias and confounding variables are minimized by the single institutional design, allowing centralized specimen procurement and clinical reports.

DOI: 10.1093/ajcp/aqy045

Other potential limitations may relate to sampling bias from the core punch method. While H&E-stained slides were used to confirm locations after core punch biopsy, the limited amount of tumor in some cases may have precluded adequate sampling (Image 1). Conversely, inadvertent contamination of infarcted regions cannot be completely excluded as cores may have inadvertently penetrated intact viable tumor or tissue. Unfortunately, the current study was not designed to analyze RNA integrity for assessment of potential sampling limitations. Finally, *BRAF*-like variants of thyroid carcinoma may express other gene fusions, not solely the *BRAF* VE600 gene mutation. Future studies are needed to address these and other potential molecular considerations.

In summary, this single-institution study characterized the clinicopathologic characteristics and histologic alterations in nine cases of thyroid carcinoma with infarction after FNA. The characterization also used NGS methods to identify hallmark *BRAF* V600E mutations (along with other known mutations) in the infarcted regions of the lesions. Analysis of residual DNA in the infarct may allow characterization by genetic mutations when absent epithelial tissue precludes diagnosis. This study comprises the second largest series characterizing malignant post-FNA lesions and demonstrates the potential utility of detection of *BRAF* V600E gene mutations in infarcted tissue.

Corresponding author: Erik Kouba, MD, Dept of Pathology, University of Alabama–Birmingham, 508 20th St South HSB 149M, Birmingham, AL35249-6823; erikjkouba@gmail.com.

Partially supported by a grant from the Department of Pathology at the University of Alabama–Birmingham.

References

1. Siegel RL, Miller KD, Jemal A. Cancer statistics, 2017. *CA Cancer J Clin*. 2017;67:7-30.
2. Cabanillas ME, McFadden DG, Durante C. Thyroid cancer. *Lancet*. 2016;388:2783-2795.
3. Riesco-Eizaguirre G, Santisteban P. Endocrine tumours: advances in the molecular pathogenesis of thyroid cancer: lessons from the cancer genome. *Eur J Endocrinol*. 2016;175:R203-R217.
4. Yoo SK, Lee S, Kim SJ, et al. Comprehensive analysis of the transcriptional and mutational landscape of follicular and papillary thyroid cancers. *PLoS Genet*. 2016;12:e1006239.
5. Fagin JA, Wells SA Jr. Biologic and clinical perspectives on thyroid cancer. *N Engl J Med*. 2016;375:1054-1067.
6. Xu B, Tuttle RM, Sabra MM, Ganly I, et al. Primary thyroid carcinoma with low-risk histology and distant metastases: clinicopathologic and molecular characteristics. *Thyroid*. 2017;27:632-640.
7. Li C, Lee KC, Schneider EB, et al. BRAF V600e mutation and its association with clinicopathological features of papillary thyroid cancer: a meta-analysis. *J Clin Endocrinol Metab*. 2012;97:4559-4570.
8. Fnais N, Soobiah C, Al-Qahtani K, et al. Diagnostic value of fine needle aspiration BRAF(V600e) mutation analysis in papillary thyroid cancer: a systematic review and meta-analysis. *Hum Pathol*. 2015;46:1443-1454.
9. Tufano RP, Teixeira GV, Bishop J, et al. BRAF mutation in papillary thyroid cancer and its value in tailoring initial treatment: a systematic review and meta-analysis. *Medicine (Baltimore)*. 2012;91:274-286.
10. Mon SY, Hodak SP. Molecular diagnostics for thyroid nodules: the current state of affairs. *Endocrinol Metab Clin North Am*. 2014;43:345-365.
11. Yip L, Sosa JA. Molecular-directed treatment of differentiated thyroid cancer: advances in diagnosis and treatment. *JAMA Surg*. 2016;151:663-670.
12. Hedegaard J, Thorsen K, Lund MK, et al. Next-generation sequencing of RNA and DNA isolated from paired fresh-frozen and formalin-fixed paraffin-embedded samples of human cancer and normal tissue. *PLoS ONE*. 2014;9:e98187.
13. Cancer Genome Atlas Research Network. Integrated genomic characterization of papillary thyroid carcinoma. *Cell*. 2014;159:676-690.
14. Haugen BR, Alexander EK, Bible KC, et al. 2015 American Thyroid Association management guidelines for adult patients with thyroid nodules and differentiated thyroid cancer: the American Thyroid Association guidelines task force on thyroid nodules and differentiated thyroid cancer. *Thyroid*. 2016;26:1-133.
15. Baloch ZW, LiVolsi VA, Asa SL, et al. Diagnostic terminology and morphologic criteria for cytologic diagnosis of thyroid lesions: a synopsis of the National Cancer Institute Thyroid Fine-Needle Aspiration State of the Science Conference. *Diagn Cytopathol*. 2008;36:425-437.
16. Richmond BK, O'Brien BA, Mangano W, et al. The impact of implementation of the Bethesda system for reporting thyroid cytopathology on the surgical treatment of thyroid nodules. *Am Surg*. 2012;78:706-710.
17. Chen JC, Pace SC, Chen BA, et al. Yield of repeat fine-needle aspiration biopsy and rate of malignancy in patients with atypia or follicular lesion of undetermined significance: the impact of the Bethesda system for reporting thyroid cytopathology. *Surgery*. 2012;152:1037-1044.
18. Cohen RN, Davis AM. Management of adult patients with thyroid nodules and differentiated thyroid cancer. *JAMA*. 2017;317:434-435.
19. Polyzos SA, Patsiaoura K, Zachou K. Histological alterations following thyroid fine needle biopsy: a systematic review. *Diagn Cytopathol*. 2009;37:455-465.
20. Liu YF, Ahmed S, Bhuta S, et al. Infarction of papillary thyroid carcinoma after fine-needle aspiration: case series and review of literature. *JAMA Otolaryngol Head Neck Surg*. 2014;140:52-57.
21. Eze OP, Cai G, Baloch ZW, et al. Vanishing thyroid tumors: a diagnostic dilemma after ultrasonography-guided fine-needle aspiration. *Thyroid*. 2013;23:194-200.
22. Kholová I. Vanishing thyroid gland tumors: infarction as consequence of FNA? *Diagn Cytopathol*. 2016;44:568-573.

DOI: 10.1093/ajcp/aqy045

23. Sharma C, Krishnanand G. Histologic analysis and comparison of techniques in fine needle aspiration-induced alterations in thyroid. *Acta Cytol*. 2008;52:56-64.
24. Baloch ZW, LiVolsi VA. Post fine-needle aspiration histologic alterations of thyroid revisited. *Am J Clin Pathol*. 1999;112:311-316.
25. Ersöz C, Soylu L, Erkoçak EU, et al. Histologic alterations in the thyroid gland after fine-needle aspiration. *Diagn Cytopathol*. 1997;16:230-232.
26. Das DK, Janardan C, Pathan SK, et al. Infarction in a thyroid nodule after fine needle aspiration: report of 2 cases with a discussion of the cause of pitfalls in the histopathologic diagnosis of papillary thyroid carcinoma. *Acta Cytol*. 2009;53:571-575.
27. American Joint Committee on Cancer. *AJCC Cancer Staging Manual*. 8th ed. New York, NY: Springer; 2017.
28. Bhatia P, Deniwar A, Mohamed HE, et al. Vanishing tumors of thyroid: histological variations after fine needle aspiration. *Gland Surg*. 2016;5:270-277.
29. Dağlar-Aday A, Toptaş B, Oztürk T, et al. Investigation of BRAF V600e mutation in papillary thyroid carcinoma and tumor-surrounding nontumoral tissues. *DNA Cell Biol*. 2013;32:13-18.
30. Kini SR. Post-fine-needle biopsy infarction of thyroid neoplasms: a review of 28 cases. *Diagn Cytopathol*. 1996;15:211-220.
31. Charles RP, Silva J, Iezza G, et al. Activating BRAF and PIK3ca mutations cooperate to promote anaplastic thyroid carcinogenesis. *Mol Cancer Res*. 2014;12:979-986.
32. Kasaian K, Wiseman SM, Walker BA, et al. The genomic and transcriptomic landscape of anaplastic thyroid cancer: implications for therapy. *BMC Cancer*. 2015;15:984.
33. Hou P, Liu D, Shan Y, et al. Genetic alterations and their relationship in the phosphatidylinositol 3-kinase/Akt pathway in thyroid cancer. *Clin Cancer Res*. 2007;13:1161-1170.
34. Santarpia L, El-Naggar AK, Cote GJ, et al. Phosphatidylinositol 3-kinase/Akt and Ras/Raf-mitogen-activated protein kinase pathway mutations in anaplastic thyroid cancer. *J Clin Endocrinol Metab*. 2008;93:278-284.
35. Landa I, Ibrahimpasic T, Boucai L, et al. Genomic and transcriptomic hallmarks of poorly differentiated and anaplastic thyroid cancers. *J Clin Invest*. 2016;126:1052-1066.
36. Ricarte-Filho JC, Ryder M, Chitale DA, et al. Mutational profile of advanced primary and metastatic radioactive iodine-refractory thyroid cancers reveals distinct pathogenetic roles for BRAF, PIK3ca, and AKT1. *Cancer Res*. 2009;69:4885-4893.
37. Park JY, Yi JW, Park CH, et al. Role of BRAF and RAS mutations in extrathyroidal extension in papillary thyroid cancer. *Cancer Genomics Proteomics*. 2016;13:171-181.
38. Jang EK, Song DE, Gong G, et al. Positive cytology findings and a negative histological diagnosis of papillary thyroid carcinoma in the thyroid: is it a false-positive cytology or a disappearing tumor? *Eur Thyroid J*. 2013;2:203-210.
39. Epstein EJ, Chao J, Keller C, et al. Infarcted papillary thyroid cancer after fine needle aspiration biopsy. *Endocrine*. 2011;40:322-323.
40. Cha YJ, Koo JS. Next-generation sequencing in thyroid cancer. *J Transl Med*. 2016;14:322.
41. Xing M. BRAF mutation in thyroid cancer. *Endocr Relat Cancer*. 2005;12:245-262.
42. Abd Elmageed ZY, Sholl AB, Tsumagari K, et al. Immunohistochemistry as an accurate tool for evaluating BRAF-V600e mutation in 130 samples of papillary thyroid cancer. *Surgery*. 2017;161:1122-1128.
43. Melck AL, Yip L, Carty SE. The utility of BRAF testing in the management of papillary thyroid cancer. *Oncologist*. 2010;15:1285-1293.
44. Kim SY, Kim EK, Kwak JY, et al. What to do with thyroid nodules showing benign cytology and BRAF(V600e) mutation? A study based on clinical and radiologic features using a highly sensitive analytic method. *Surgery*. 2015;157:354-361.
45. Swierniak M, Pfeifer A, Stokowy T, et al. Somatic mutation profiling of follicular thyroid cancer by next generation sequencing. *Mol Cell Endocrinol*. 2016;433:130-137.
46. Vuong HG, Altibi AM, Abdelhamid AH, et al. The changing characteristics and molecular profiles of papillary thyroid carcinoma over time: a systematic review. *Oncotarget*. 2017;8:10637-10649.
47. Walts AE, Pao A, Sacks W, et al. BRAF genetic heterogeneity in papillary thyroid carcinoma and its metastasis. *Hum Pathol*. 2014;45:935-941.
48. Durante C, Tallini G, Puxeddu E, et al. BRAF(V600e) mutation and expression of proangiogenic molecular markers in papillary thyroid carcinomas. *Eur J Endocrinol*. 2011;165:455-463.
49. Jolly LA, Novitskiy S, Owens P, et al. Fibroblast-mediated collagen remodeling within the tumor microenvironment facilitates progression of thyroid cancers driven by BrafV600E and Pten loss. *Cancer Res*. 2016;76:1804-1813.
50. Sun WY, Jung WH, Koo JS. Expression of cancer-associated fibroblast-related proteins in thyroid papillary carcinoma. *Tumour Biol*. 2016;37:8197-8207.
51. Nucera C, Lawler J, Parangi S. BRAF(V600e) and microenvironment in thyroid cancer: a functional link to drive cancer progression. *Cancer Res*. 2011;71:2417-2422.
52. García-Rostán G, Costa AM, Pereira-Castro I, et al. Mutation of the PIK3ca gene in anaplastic thyroid cancer. *Cancer Res*. 2005;65:10199-10207.
53. Xu B, Ghossein R. Genomic landscape of poorly differentiated and anaplastic thyroid carcinoma. *Endocr Pathol*. 2016;27:205-212.

DOI: 10.1093/ajcp/aqy045